Thermopile IR Sensor Arrays

V.A. Fedirko, E.A. Fetisov, R.Z. Khafizov, G.A. Rudakov and A.A. Sigarev

Abstract Thermopile thermo-sensitive element for infrared (IR) sensor array and its optimization is considered. A concept of thermal infrared sensor array based on the micro (nano)-electromechanical system (MNEMS) with nonstationary Seebeck effect is discussed. Infrared absorption of non-stoichiometric silicon nitride thin films has been studied in the region of wavenumbers 500–7500 cm^{-1}. The estimated absorption about 64% is found for 1300 nm layer thickness, which is good enough for thermal sensor.

Keywords Thermal sensor array · Thermopile · Infrared absorption

V.A. Fedirko
National Research University of Electronic Technology "MIET",
Moscow State University of Technology "Stankin" (MGTU "Stankin"),
Moscow, Russia
e-mail: vfed@mail.ru

E.A. Fetisov (✉) · R.Z. Khafizov
National Research University of Electronic Technology "MIET", Moscow, Russia
e-mail: fetisov@inicm.ru

R.Z. Khafizov
e-mail: imagelab@mail.ru

G.A. Rudakov
SMC Technological Centre, Zelenograd, Russia
e-mail: grigory.rudakov@gmail.com

A.A. Sigarev
Moscow Institute of Physics and Technology (State University), Moscow, Russia
e-mail: aasigarev@mail.ru

K.V. Anisimov et al. (eds.), *Proceedings of the Scientific-Practical Conference "Research and Development - 2016"*, https://doi.org/10.1007/978-3-319-62870-7_5

Introduction

Uncooled infrared (IR) imagers [1, P.203; 2, P.66; 3, P.99] have attracted a great deal of interest due to their wide range of practical applications. Their greatest advantage is that they do not need expensive deep cooling systems in contrast to semiconductor quantum infrared photodetectors. In recent years, thermopile IR imager arrays have been actively developed on the base of MEMS technology, which is compatible with the silicon CMOS batch technology [4, P.200; 5, P.239; 6, P.42; 7, P.49]. A sensitive MEMS element comprises an IR high-absorbance dielectric membrane and micro-thermopiles, with the hot contact laying on the membrane and the cold one being in a good heat contact with the substrate. The output voltage of the thermopile, which is generated during the membrane heating (Seebeck effect) is read out by CMOS circuit, which is formed directly on the same chip. Good thermal isolation and low thermal capacity of thermopile-based MEMS elements are the good foundations for the development of uncooled thermal IR-image sensors with high sensitivity, linearity, low power consumption, and high responsivity. Micro-thermocouples are fabricated from polysilicon that ensures sufficiently high thermo-power while their conductivity and thermo-power can be adjusted by the proper doping. Besides, polysilicon is technologically well-proven and widely used material in CMOS technology, which makes it possible to form the sensitive elements and the electronic readout circuit in one chip, to produce efficient imagers and to reduce the production cost.

In this paper, we discuss some aspects of the optimal design and study of MEMS thermopile IR-sensors.

Optimal Design of MEMS Thermopile Element for IR Imager Array

Figure 1 shows schematically a MEMS thermopile element for IR imager array.

The membrane with IR-absorbing layer is suspended on the microcantilevers made of an electro-isolating material with low thermal conductivity. The thermopile is built on the cantilever surface, one contact of the thermopile is heated by the membrane, and the other contact is placed on the silicon substrate with a stable temperature. The output voltage of thermopile is read out by the CMOS integrated

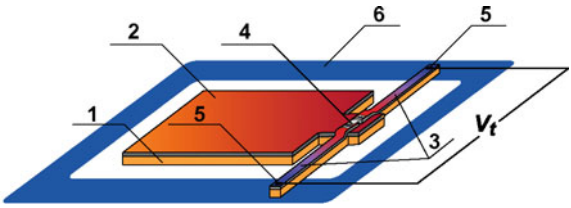

Fig. 1 Principal scheme of the MEMS thermopile element. *1* membrane; *2* absorbing layer; *3* cantilevers with thermopile; *4* hot contact; *5* cold contacts; *6* substrate

circuit, which is formed directly on the chip. The actual structural design can be easily reduced to that arrangement. The membrane and the cantilever beams are formed on a silicon wafer and made, for example, of thermal silica dioxide. SiN_x layer may serve as an IR-absorbing material which provides quite effective IR absorption in the specified wavelength region of 8–14 μm. The thermopile is made of anisotype (*p* and *n*-doped) polysilicon buses which are characterized by sufficiently high Seebeck coefficient. The process technology of this MEMS sensor is well compatible with standard CMOS batch technology. Vacuum-sealed package design is supposed to prevent from heat sink through the gas atmosphere.

When designing the IR sensor array, the following key parameters should be taken into account: the number N of sensor elements in the array for the required spatial resolution, frame time τ_f defining the time resolution, and preassigned minimal resolved temperature difference at the object δT_m.

The output characteristic of the thermopile is the open-circuit voltage (output voltage) which for the variable signal on the frequency f is defined by the well-known expression:

$$\Delta V_f = \frac{\alpha \cdot \Delta P_f \tau}{C\sqrt{1 + (2\pi f \tau)^2}}, \tag{1}$$

where α is the Seebeck coefficient of the thermopile, ΔP_f is the corresponding frequency component of the IR emission from the object absorbed by the sensor, C—it's heat capacitance. According to Kotelnikov theorem [8, P.736], the width of the reconstructed spectrum of the variable signal by discrete processing equals a half of the sampling frequency. That restricts the thermal relaxation time τ of the sensitive element by:

$$\tau \leq \tau_f / \pi. \tag{2}$$

Thermal relaxation time of the element is defined by the membrane thermal capacitance and the thermal conductivity of thermopile G_t:

$$\tau \approx C / G_t. \tag{3}$$

The intrinsic noise of a thermopile is defined by Johnson noise of its resistance R that provides the following value of the noise-equivalent temperature difference (NETD) of the object:

$$\mathrm{NETD} = \frac{2C \cdot \sqrt{k_B \mathrm{TBR}}}{\alpha \cdot (\Delta p / \Delta T) \cdot A \cdot \tau} < \delta T_m, \tag{4}$$

where k_B is the Boltzmann's constant, T is the ambient temperature, B is the bandwidth of the readout circuit, A is the area of the absorber, Δp is the excess IR radiation power of black body heated to temperature $T + \Delta T$, absorbed by sensor

located in the focal plane of the optical system of the imager. Equations (3) and (4) demonstrate that the lowest NETD of such sensitive MEMS thermopile element is achieved in the structure with single thermopile: serial connection of thermopiles does not result in the increase of the open-circuit voltage of the element because the membrane heating is reduced proportionally due to the increase of total thermal conductivity. At the same time, the total electrical resistance is increasing according to (3), resulting in the increase of NETD.

The number of array elements at a certain size of the chip limits the maximal area of the cell and, respectively, the area S of the thermal sensor itself. The area of the sensor as seen from Fig. 1 is shared between the area of the membrane A and the cantilever area A_c:

$$S = A + A_c; \quad A_c = 2\mu w_t \cdot l, \tag{5}$$

where w_t is the length of one shoulder of the thermopile, l is the length of the cantilever, μ is the "adjacent" coefficient to take the space distances into account.

Thermopile conductivity and its electrical resistance are defined by the formulae, respectively:

$$G_t = \frac{2k_t w_t h_t}{l}, \quad R = \frac{2\rho_t l}{w_t h_t}, \tag{6}$$

where h_t is the thickness of thermopile material (polysilicon), k_t is the thermal conductivity coefficient of the thermopile material, ρ_t is its resistivity (assuming that both shoulders of the thermopile have similar resistance values). Optimization of the structure geometry is then achieved by minimizing the NETD over the variables A and l when:

$$A + 2\mu w_t \cdot l = S, \quad \tau = \frac{cAl}{2k_t w_t h_t} \le \tau_f/\pi, \tag{7}$$

where c is the thermal capacitance of membrane unit area. That gives [9, P.59; 10, P.125029]:

$$A = \frac{2}{3}S, \quad A_c = \frac{1}{3}S, \quad l = \frac{S}{6\mu w_t}. \tag{8}$$

For a specified τ it can be implemented providing:

$$S \ge 4\sqrt{k_t \mu w_t^2 h_t \tau / c}, \tag{9}$$

that determines the minimal possible area of the sensor for a given τ with all other parameters of the structure being fixed. Vice versa, the maximal thermal relaxation time τ which can be implemented at the specified sensor area S can be expressed as follows:

$$\tau \leq \frac{cS^2}{16k_t\mu w_t^2 h_t}. \tag{10}$$

The lowest NETD and the highest open-circuit voltage are reached according to (1) and (3) at the maximal value of thermal relaxation time of the sensor permitted by (2): $\tau = \tau_f/\pi$. However, it can be realized according to (9) providing that:

$$S = S_{\text{opt}} = 3 \cdot \sqrt{2k_t\mu w_t^2 h_t \tau_f/\pi c}, \tag{11}$$

with optimal ratio of the membrane and cantilever areas (8). The corresponding optimized NETD value is as follows:

$$\text{NETD} = \frac{6(k_t w_t h_t)\sqrt{6\mu k_B T r_\square}}{\alpha\eta q j \cdot S_{opt}^{3/2}\tau_f^{1/2}} = \frac{2 \cdot \sqrt{k_B T \rho_t}}{\alpha\eta q j \tau_f^{5/4}} \cdot (\pi c)^{3/4} \cdot \left(\frac{k_t}{2\mu w_t^2 h_t}\right)^{1/4}. \tag{12}$$

Here we take into account that $(\Delta p/\Delta T) = \eta q j$, where η is the part of incident IR emission absorbed by the membrane in the covered spectral range, q is the optical factor: $q = Ht_o/4$, where H is the lens aperture and t_o is the transmission factor of the lens, $j \approx 2.62$ W/m^2 K for the 8 ÷ 14 μm wavelength region; also we assume, in accordance with the above mentioned, that $r_\square = \rho_t/h_t B = 1/2\tau_f$, and we introduce the thermopile sheet resistance .

NETD (12) should satisfy inequality (4), and the optimized area of sensor should not exceed S_p, determined by the specified structural design of the IR imager and the chip size S_c: $S \approx S_p \leq S_c/N$. Hence, to achieve the preassigned resolving temperature difference at the object δT_m for the specified structural design and for the frame time τ_f, the parameters of the element should meet the following requirement:

$$\frac{k_t w_t \sqrt{\mu\rho_t h_t}}{\alpha\eta q} < \frac{j\tau_f^{1/2}\delta T_m}{6\sqrt{6k_B T}} \left(\frac{S_c}{N}\right)^{3/2}. \tag{13}$$

Until the size of the array is not very large so that $S_p > S_{\text{opt}}$, the ratio $\chi = A/S$ is restricted by (2): $\tau = \tau_f/\pi$, that results in the expression:

$$\frac{9}{2}\chi(1-\chi) \cdot \left(S/S_{\text{opt}}\right)^2 = 1, \tag{14}$$

thus, the optimized ratio χ, evidently, cannot be achieved. Here, as S becomes lower, NETD increases as $\sim S^{-1/2}$. For large-size arrays with $S_p \leq S_{\text{opt}}$, the maximal relaxation time according to (10) is $\tau \leq \tau_f/\pi$ and $\tau \sim S^2$. The lowest NETD is achieved according to (8) when $\chi = 1/3$, but now the NETD increases much rapidly with the reduction of the element area: NETD $\sim S^{-3/2}$. As a result, the element operational parameters significantly worsen at $S < S_{\text{opt}}$ and that should be taken into account when designing large format imagers arrays with $S_p \leq S_{\text{opt}}$.

One can see from (13) that the element technology is faced with higher demands when enlarging the array size, the frame frequency, and the temperature difference resolution. The necessary characteristics can be achieved following Eq. (14) by reducing the width and the thickness of the thermopile, by increasing the absorption capacity of the IR imager and by optimizing the ratio $\sqrt{\rho_t}/\alpha$. When $h_t = 0.1$ μ, $w_t = 1$ μ, $c = 2$ J/m^2 K, $\mu = 2.5$, with $\alpha = 300$ μV/K, $r_\square = 20$ O, $\eta = 0.8$, $H = 1$, we find for $\tau_f = 0.05$ s:

$$S_{\text{opt}} \approx 1500\,\mu^2, \quad \text{NETD} \approx 8.5\text{m}\kappa \tag{15}$$

That makes it possible to develop, for example, a 128 × 128 array with 50–60 μm pitch and high-temperature resolution. Note, however, that to register such a signal its pre-amplification directly in the cell should be performed followed by the signal processing in the integrated circuit formed directly on the chip [11, P.1701].

Switchable Thermopile Sensor

A chance to increase the efficiency of thermal imagers with slower response time can be provided by a sensor with switchable thermopile [12, P.596]. In a photosensitive MEMS element of that type, the cold thermojunction is not in a permanent contact with the substrate while the membrane is suspended on additional supporting SiO_2 consoles (are not shown in Fig. 1). The thermopile has cold contacts capable of closing and opening under the effect of elastic and electrostatic forces, the equilibrium contact gap in the open state is supposed to be $\sim 100 \div 500$ nm. The switching process in such a system under the applied voltage is described, e.g., in [2, P.66]. As the thermal conductivity of SiO_2, G_c, is about 30 times lower than that of the polysilicon thermopile, the heat sink from the membrane through the supporting SiO_2 consoles is very small when the thermopile is disconnected from the measurement circuit, while for measuring the output thermo-power the contacts close for a short measuring time τ_r only. The membrane heating temperature (and hence the temperature of hot thermojunctions) in the open cold contact state is then limited by the thermal relaxation time $\tau_0 \approx C/G_c$ which is substantially higher than the relaxation time τ_t when the cold thermojunction is in permanent thermal contact with the substrate. That's why the heating of the membrane may markedly exceed its heating in an ordinary element discussed above. Yet the response time of such an element decreases to the same extent. Nevertheless, providing the same characteristics, the length of the supporting SiO_2 console is much shorter. That allows increasing of the filling factor of an element area S_p with the photosensitive membrane and thus reduces S_p which gives a possibility to increase, in principle, the format of the imager. This is also the way to reduce the time of τ_m of the mechanical switching to $\tau_m \ll \tau_f$. At the same time that makes it possible to shorten the length of the thermopile and thus reduce its intrinsic noise due to the reduction

of its resistance providing, of course, that the length of the thermopile in the closed cold contact state ensures the cooling time of the membrane $\tau_t \gg \tau_r$.

Obviously, a nonstationary Seebeck effect is, generally speaking, observed in such an element. The required dynamic of thermal and electrical processes in the sensor array with a switchable thermocouple and SiO_2 consoles is determined by the following hierarchy of characteristic times:

$$\tau_{p,n} < \tau_1 < \tau_m < \tau_r \ll \tau_t \ll \tau_0 \leq \tau_f/\pi. \tag{16}$$

Here $\tau_1 \approx (\rho c l^2/\pi^2 k_t)$ is the intrinsic thermal relaxation time of the thermopile, and $\tau_{p,n} \sim l^2/D$, ρ being the density, c is the thermal capacitance and k_t is the thermal conductivity of the thermocouple material (polysilicon), l is the length of the thermopile and D is the diffusion coefficient of charge carriers in it. If (16) is realized, the quasi-stationary state of the thermopile is established in the short time τ_1 when the cold contact of the thermopile comes into the contact with the substrate, and the temperature difference $\Delta T \approx \Delta P \tau_0/C$ at the thermo-junctions is registered by measuring circuit before it diminishes to $\Delta T \approx \Delta P \tau_t/C$.

For an element with the SiO_2 the console length of 100 μ, the width of 2 μ and the thickness of 0.5 μ, with the membrane area of 5000 mm^2 and the thermopile length of l = 100 μ, we find: $\tau_0 \approx 1$ s, $\tau_t \approx 0.03$ s, $\tau_1 \approx 5 \times 10^{-7}$ s, $\tau_{p,n} \approx 10^{-7}$ s that satisfy the conditions (17). The measured output voltage of the thermopile is then:

$$\Delta V = \alpha \cdot \Delta T \approx \frac{\alpha \cdot \Delta P}{C} \tau_0 \gg \frac{\alpha \cdot \Delta P}{C} \tau_t. \tag{17}$$

The open-circuit voltage of such an element, as one can see, may significantly exceed the output voltage of an ordinary sensor. However, it is achieved through the corresponding enlarging of the response time of the element which is τ_0 here, so the frame time τ_f can be no less than 3 s.

Therefore, the vacuum IR sensor array with "switchable" thermopiles can be quite effective for the "slow" thermal imaging systems. It may also serve as an alternative to a conventional sensor and quick-response large format systems when a small area of an element limits the length of the thermopile and does not ensure the optimal thermal relaxation time but the technology cannot provide it by reducing its thickness and width. It should be mentioned, however, that the implementation of the proposed elements may face some design, technological and circuit problems.

Study of Non-stoichiometric SiN_x Layers

Silicon nitride is considered to be the possible material for producing of thermo-sensitive elements. With an intensive IR absorption band related to the Si–N stretching vibrations in the 700–1100 cm^{-1} wavenumbers region with the peak at

820–900 cm^{-1} corresponding to the atmospheric 8–14 μm transparency window, SiN_x provides a chance to combine, in principle, the function of supporting membrane of the sensing element and the heat absorber in one material. The PECVD non-stoichiometric SiN_x films possess lower and well-controllable internal stress with good mechanical properties as compared to the stoichiometric Si_3N_4 films. That enables to use SiN_x films in fabrication of membrane elements and consoles for the IR thermo-sensitive micro-detectors [13, P.58].

We have studied the SiN_x layers with thicknesses from 200 to 1300 nm produced by plasma enhanced chemical vapor deposition (PECVD) on monocrystalline silicon wafers.

The measurements of IR transmittance T and reflectance R spectra in the region of wavenumbers v = 500–7500 cm^{-1} were taken on Fourier transform spectrometer "Perkin-Elmer Spectrum 100." The reflectance spectra were measured at the incidence probing IR radiation both on the front surface of the wafer with SiN_x and on the back surface of the wafer without SiN_x. Figure 2 shows the spectral functions:

$$A(v) = -\log 10(T(v)/T_0(v)), \tag{18}$$

estimated by the ratio of the transmittance spectra of the spectrometer channel with the sample $T(v)$ and without the sample (an empty spectrometer channel) $T_0(v)$ for the analyzed samples.

To estimate the absorption of SiN_x films in the above IR band region, the reflectance spectra of the samples were analyzed. For this purpose, thick Al layer

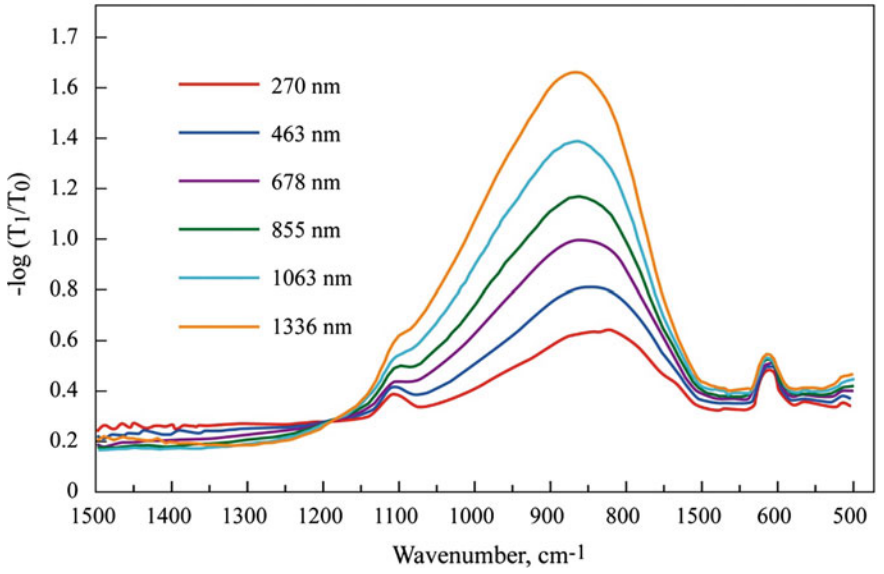

Fig. 2 Spectral functions of absorbance spectra A(v) for SiN_x layers with thicknesses: *1* 270 nm; *2* 463 nm; *3* 678 nm; *4* 855 nm; *5* 1063 nm; *6* 1336 nm

was deposited on the backside of the wafer. The reflectance spectra observed in the 700–1150 cm^{-1} region (9–14 μm) were about $R \sim 35\%$ for the thick SiN_x film (1336 nm) and about $R \sim 55\%$ for thin film (270 nm). The part of absorbed radiation can be estimated as $A \approx 1 - R$, that is equal to $\sim 65\%$ for thick SiN_x film (1336 nm) and to $\sim 45\%$ for the thin SiN_x film (270 nm). Taking into account the double way of IR radiation through the SiN_x film, the one-way absorption A_1 is approximately estimated by the equation $A \approx A_1 + A_1(1 - A_1)$, from that one finds $A_1 \approx 1 - \sqrt{1 - A}$ which gives $A_1 \approx 40\%$ for a thick layer sample and $A_1 \approx 26\%$ for a thin layer sample.

The results allow concluding that the optimal thickness of SiN_x film for effective thermal detection is $1.0 \div 1.5$ μ.

Conclusion

Optimal engineering of a thermopile thermal MEMS element for IR sensor array is considered. Theoretical relations are obtained which optimize the sensor structure to achieve the preassigned characteristics of an imager array such as image format, frame time and temperature difference resolution. Thermal sensor with nonstationary Seebeck effect using "switchable" thermocouple is analyzed. Non-stoichiometric silicon nitride thin films have been studied as an IR absorption layer and are shown to be good enough for use for thermopile thermal MEMS thermosensors.

Acknowledgements Research was carried out with the financial support of the state represented by the Ministry of Education and Science of the Russian Federation. Agreement no. 14.578.21.0009 05 June 2014. Unique Project Identifier: RFMEFI57814X0009 and was partially supported by the Russian Foundation for Basic Research, project No. 15-07-06082-a.

Authors thank L.B. Sharova for critical reading of the manuscript.

References

1. Kruse, P.W., Skatrid, D.D. (eds.): Uncooled Infrared Imaging Arrays and Systems. Semiconductors and Semimetals, 347 p. Academic Press, USA (1997)
2. Fedirko, V.A., Fetisov, E.A., Bespalov, V.A.: Termomechanical nanomembrane IR-imaging sensors. Prikladnaya Fizika (Appl. Phys.). **1**, 66–72 (2010) (in Russian)
3. Fedirko, V.A., Fetisov, E.A., Svidzinsky, K.K.: Performance limit of infra-red thermomechanical imager with optical readout. Univ. J. Appl. Sci. **2**(5), 99–103 (2014)
4. Schaufelbuhl, A., Munch, U., Menfoli, C., Brand, O., Paul, O., Huang, Q., Baltes, H.: 256-pixel CMOS-integrated thermoelectric infrared sensor array. 2001 IEEE MEMS 2001 Conference, pp. 200–203. Interlaken, Switzerland, 21–25 January 2001 (2001)
5. Hirota, M., Nakajima, Y., Saito, M., Satou, F., Uchiyama, M.: 120×90 element thermopile array fabricated with CMOS technology. Proceedings of SPIE Conference, Infrared Technology and Applications XXVIII, vol. 4820. pp. 239–249, 23 January 2003

6. Forg, B., Herrmann, F., Schieferdecker, J., Leneke, W., Schulze, M., Simon, M., Storck, K.: Thermopile sensor array with improved spatial resolution, sensitivity and image quality. Sens. Test Proc., pp. 42–44. Nürnberg, Germany (2011)
7. Khafizov, R.Z.: Infrared Focal Plane Array (FPA) with termopile thermal radiation MEMS sensors. Proceedings of VI All-Russia Science & Technology Conference MES-2014, Extended abstracts, Part II, Institute for Design Problems in Microelectronics of Russian Academy of Science, pp. 49–55. IPPM RAS, Moscow (2015)
8. Kotel'nikov, V.A.: On the transmission capacity of 'ether' and wire in electric communications (1933). Phys. Usp. **49**, 736–744 (2006)
9. Fedirko, V.A., Khafizov, R.Z., Fetisov, E.A.: Optimal design of the MEMS thermopile element for an IR imager array. In: Stempkovsky, A. (ed.) Problems of Perspective Micro- and Nanoelectronic Systems Development—2016, Part IV. pp. 59–64. IPPM RAS, Moscow, 3–7 October 2016 (2016)
10. Xie, J., Lee, C., Wang, M., Liu, Y., Feng, H.: Characterization of heavily doped polysilicon films for CMOS-MEMS thermoelectric power generators. J. Micromech. Microeng. **19**(12), 125029–125036 (2009)
11. Wang, J.-Q., Shen, C.-H.: An offset reduction infrared tracking system with winner-take-all implementation for CMOS thermal microsensor. IEEE Sensors Conference, pp. 1701–1704 (2009)
12. Fetisov, E.A., Fedirko, V.A., Timofeev, A.E.: Study of thermal IR sensor on the base of vacuum micro/nanoelectromechanical system with non-stationary thermocouple's Seebeck effect. Proceedings of the 2016 International Conference on Actual Problems of Electron Devices Engineering, Saratov, vol. 2. pp. 596–601, 22–23 September 2016 (2016) (in Russian)
13. Rudakov, G.A., Sigarev, A.A., Fedirko, V.A., Fetisov, E.A.: Characterization of non-stoichiometric silicon nitride PECVD/ALD films for micro-detectors of IR imager array. Proceedings of 14th International Baltic Conference on Atomic Layer Deposition (BALD-2016), Book of Abstracts, S.-Petersburg, p. 58, 2–4 October 2016 (2016)